Ontogenetic Changes of the Water Status and Accumulated Soluble Compounds in Growing Cherry Fruits Studied by NMR Imaging

N. Ishida,[1]* H. Ogawa,[2] M. Koizumi[3] and H. Kano[3]
[1] National Food Research Institute, Tsukuba Science City, Ibaraki 305, Japan
[2] JEOL Datum, Akishima, Tokyo 196, Japan
[3] National Institute of Agrobiological Resources, Tsukuba Science City, Ibaraki 305, Japan

Ontogenetic changes of water status and accumulated soluble compounds in growing cherry fruits were examined by ^{1}H NMR imaging, ^{1}H NMR localized spectral imaging and ^{13}C NMR spectroscopy. Water status was contradictory between the seed and pericarp of the fruit in relation to growth stages. There was a large amount of high-mobility water present in the seed, whereas only a small amount was present in the pericarp during the early growth stages. The diffusion coefficient of seed water was determined as 2.1×10^{-5} cm^2 s^{-1} at the maximum, which corresponded to that of pure water (2.14×10^{-5} cm^2 s^{-1} at 25 ± 1 °C). Water in the seed decreased in amount and mobility whereas that in the pericarp increased with maturation. The diffusion coefficient of pericarp water increased from 1.0×10^{-5} to 1.6×10^{-5} cm^2 s^{-1} as the fruit ripened. Sugars accumulated in the pericarp with increasing water content, but disappeared with further ripening of the fruit. This suggests that over-maturation results in loss of sweetness and firmness. NMR imaging could probe changes in the physiological condition of the fruit with growth stages. © **1997 John Wiley & Sons, Ltd.**

Magn. Reson. Chem. **35**, S22–S28 (1997) No. of Figures: 5 No. of Tables: 2 No. of References: 36

Keywords: NMR; ^{1}H NMR; ^{13}C NMR; sweet cherry fruits; cell-associated water; imaging; spin–lattice relaxation time; diffusion coefficient

Received 4 April 1997; revised 16 July 1997; accepted 16 July 1997

INTRODUCTION

The cherry fruit is a seasonal product of early summer. The fruit has a flavorful and sweet taste, and also has a soft and elastic texture. The quality of the cherry is related to the tree condition and degree of maturation, in addition to solar irradiation and temperature. Therefore, skilful and elaborate cultivation is needed to obtain good-quality fruits. In addition, the fruit is difficult to preserve for long periods of time; the characteristic taste, firmness and sweetness are quickly lost.[1] The reason for the degradation of the fruits and measures for preventing this degradation have never been thoroughly investigated. Investigating the timing of harvesting and improving conditions for fruit quality preservation during commercial processes[2,3] may make the fruit more common to the consumer.

Magnetic resonance imaging (MRI) or NMR imaging is a useful means for examining physiological conditions and quality of fruits. NMR imaging probes free water without destroying tissues organizations.[4,5] Since cell-associated water is closely related to cell metabolism and growth,[6,7] physiological differences in individual tissues can be detected by NMR imaging in plants. Faust *et al.*[8] studied the dormancy of apple buds and Gardea *et al.*[9] winegrape; both groups showed that free water was absent in winter-dormant buds but present in summer-dormant buds. Wang *et al.*[10] detected a water core in apple fruits and Wang and Wang[11] traced core breakdown in pear fruits. The metabolic intermediates and secondary metabolites accumulated in the tissues are detected by NMR imaging; the compounds are closely related to the taste of fruits. Pope[12] examined sugar localization in grape-berry fruits by chemical shift imaging. The amount and movement of free water provide information about the structural frame and the properties of the interface of water spaces;[13–15] these are important factors that determine the integrity and textural feel of fruits. Ishida *et al.*[16] stated that changes in water status after coloring are important in determining the taste and texture of cherry tomato fruits. Sonego *et al.*[17] observed the weakening of the proton signal with the woolly breakdown of nectarines, which was ascribed to the development of gas spaces in the tissues.

In this investigation, ontogenetic changes in water status and accumulated soluble compounds in growing sweet cherry fruits were studied by ^{1}H NMR imaging combined with ^{1}H NMR localized spectral imaging and ^{13}C NMR spectroscopy, for a better understanding of the physiology of the fruit in relation to cultivation.

* *Correspondence to*: N. Ishida.

 CCC 0749–1581/97/SI0022–07 $17.50

EXPERIMENTAL

Plants

Sweet cherry (*Prunus avium* L. cv. Sato-Nishiki) plants were grown by soil culture in 13 l pots using 10 g of 8–3.5–6.5 (N–P–K) chemical fertilizer and 5 g of $Ca(NO_3)_2$ together with organic manure in a greenhouse at 30 °C during the day and 25 °C at night. Fruit size was reduced by increasing fruit production and irrigation control in order to place the sample in a 10 mm sample holder of an NMR micro-imaging probe. Although the fruit size was small compared with that in markets, the characteristics of the fruits were maintained. Flowering began on March 29. Fruits were harvested at various growth stages, on April 10, 12, 14 and 22 and May 6, and then subjected to NMR measurements. Growth stages were determined mainly from fruit sizes, taking into account growing days after flowering and labeled first, second, third, mature and ripened. The first stage was the early rapid growing stage, the second stage was the intermediate slow growing stage and the third stage was the late rapid growing stage of the fruits. The mature and the ripened stages were essentially included in the third stage. The top of the fruits colored at the mature stage and the fruits were red at the ripened stage.

NMR imaging and NMR spectroscopy

An NMR spectrometer (Model GSX-270, JEOL, Akishima, Tokyo, Japan) operating at 270 MHz for ^{1}H and an NMR micro-imaging probe devised by Ishida *et al.*[18] were used. An intact cherry fruit was fixed on the sample holder and set in the micro-imaging probe with a detector of 15 mm diameter. The probe was equipped with a gradient coil for producing magnetic field gradients (up to 278 mT m^{-1}). The spin-echo two-dimensional Fourier transform method was used for imaging [Fig. 1(a)]. The echo time was 21 ms and four acquisition transients were accumulated. Images were created on a 256 × 256 matrix by an image processor (JEOL GIM-270) resulting in a resolution of 0.05 mm × 0.05 mm and 1.6 mm slice thickness (0.004 mm^3). Six imaging pulse sequences with different repetition times (0.5, 0.9, 1.2, 1.5, 2.0 and 5.0 s) were used to estimate spin–lattice relaxation times (T_1) of water by the progressive saturation method.[19] The values were obtained by the non-linear least-squares method with a simple exponential function using the T_1-weighted image data and images of the calculated T_1 values (T_1 image) were created using a microcomputer (PC 9801, NEC, Tokyo, Japan) and an image analyzer (AVIO SPICCA II, Nippon Avionics, Tokyo, Japan).

A localized spectral imaging method was employed to detect effectively small sugar signals vicinal to the large water signal in place of chemical shift imaging and the localized spectral image was combined with the corresponding ^{1}H NMR image to locate the sugars and oils. Localized ^{1}H NMR spectra were measured by selectively exciting a narrow central area of the fruit transversely.[16] The water signal was suppressed by using a

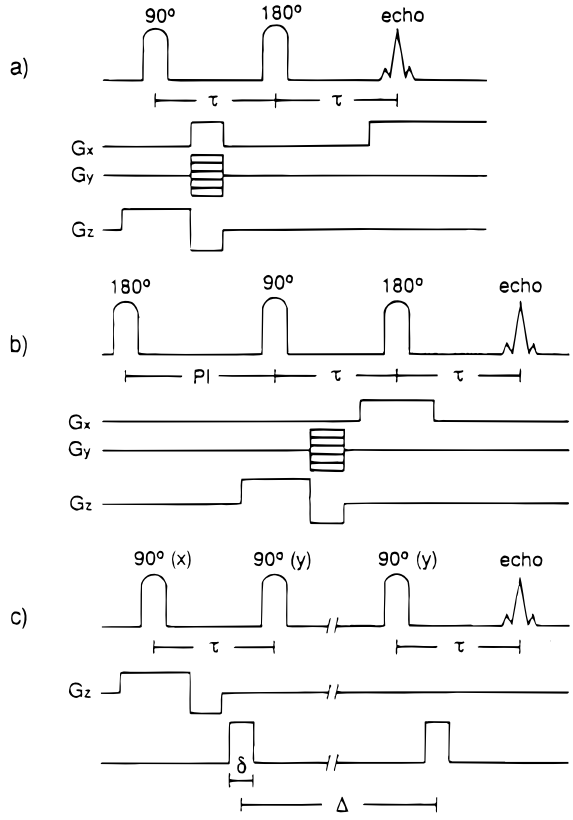

Figure 1. Pulse sequences for (a) ^{1}H NMR imaging, (b) localized spectral imaging and (c) restricted diffusion measurement. Sequence (a) is ordinary spin–echo two-dimensional Fourier transform imaging technique. The *y*-axis encoding is removed and the central area of the *x*-axis is selectively excited vertically at 180° r.f. pulse in sequence (b). A 180°–90° pulse sequence is used for excitation with water suppression (b). Sequence (c) is a pulse gradient stimulated-echo method. Symbols in the sequences are as follows; **Δ**, diffusion time; **δ**, duration of pulse magnetic field gradients; τ, half of echo time.

180° and 90° pulse sequence[20] [Fig. 1(b)]. Spectral data for 16 acquisition transients were accumulated and the results are indicated as localized spectral images, in which the *x*-axis is chemical shift and the *y*-axis the vertical position on the central area of the fruits.

Strong magnetic field gradients (278 mT m^{-1} for 3 ms) were applied for measurements of restricted diffusion using the pulse gradient stimulated-echo method[14,21] with a varying diffusion period [Fig. 1(c)]. The echo time was 27 ms and data for four acquisition transients were accumulated. After Fourier transformation, data were transferred to the microcomputer and diffusion coefficients, compartment (water space) size and the permeability of membrane partitions consisting of the compartments were calculated. All measurements were carried out at 25 ± 1 °C.

^{13}C NMR spectra of an intact fruit and 80% ethanol extract of pericarps

Pericarps of the mature stage were homogenized in twice the volume of 80% ethanol. Cell debris was discarded by centrifugation at 10 000*g* for 15 min. The supernatant was vacuum evaporated below 40 °C and dried and then 2 ml of D_2O were added. ^{13}C NMR

spectra were measured with the same spectrometer as used for imaging, adjusting the resonance frequency to 67.9 MHz. The pulse angle was 45° and the repetition time was 2.6 s with 1000 acquisition transients. Chemical shifts of the signal were referred to a standard compound (tetramethylsilane) in a capillary tube which was inserted into the sample tube. The peaks were assigned to compounds according to the chemical shifts of the signal compared with the spectra of standard compounds (Sigma, St Louis, MO, USA).

An intact fruit or a seed at the ripened stage was placed in a 10 mm sample tube then subjected to ^{13}C NMR measurements according to the above method with a 1.0 s repetition time and 20 000–50 000 acquisition transients. Measurements were carried out at 25 ± 1 °C.

RESULTS

NMR imaging detects mobile water, free water in tissues which is simply called water in this investigation. A ^{1}H NMR image (Fig. 2, left) indicates the anatomy of the fruit at the ripened stage. Typical ^{1}H NMR images (left), ^{1}H NMR localized spectral images (center) and images of calculated T_1 values (T_1 image) (right) of growing cherry fruits are shown in Fig. 3. The ^{1}H NMR images show different tendencies in changes of water status between seeds and pericarps of the fruit. There were large amounts of free water in the seeds until the third stage when the fruit size reached approximately 80% of that of the ripened stage. During this time, water was observed in the shells. Water in the seeds subsequently decreased with seed maturation associated with accumulation of stored materials. A water signal was not observed with the seed at the ripened stage, although it contained approximately 60% water on a fresh weight basis. On the other hand, there were small amounts of water in the pericarps of the young fruits. The amount of water in the pericarp increased after the mature stage, while the water content decreased in the seed. Finally, large amounts of water accumulated in the pericarp. In the epidermal tissues, large amounts of water was found after the second stage.

^{1}H NMR localized spectral images are indicated as chemical shifts of signals on the x-axis and the corresponding y-axis position on the left image on the y-axis. The water signal was suppressed for the clear detection of small amounts of sugars. Sugars (indicated by arrows s) were at first accumulated in pericarp with increase in water content at the mature stage but disappeared at the ripened stage. While oils were detected in the seed of the over-mature fruit (indicated by an arrow o).

The T_1 images show that water in the seeds increased in mobility until the third stage when the seeds contained large amounts of water. The mobility of water in the seeds declined at the mature stage. In contrast to the seeds, the mobility of water in the pericarp was low until the third stage when there were small amounts of water present. It increased at the mature and the ripened stages associated with increase in amount of water. The T_1 values in individual tissues of the fruits are listed in Table 1. The T_1 values in the seeds at the second and third stages were approximately 2 s, whereas the T_1 values of the pericarps at these stages were short. The T_1 values decreased to 0.5 s in the seeds but increased to 1 s in the pericarp at the mature stage.

Restricted diffusion of cell-associated water was measured in order to determine the organization of the tissues by the pulse gradient stimulated-echo method [Fig. 1(c)]. In the experiment, the imaging technique was not used and the signal came from all areas of a sliced section with various tissues containing various states of water. Therefore, the properties of water in individual tissues cannot be determined; however, considering the results in Fig. 3, the signals mainly came from the seeds until the third stage and from the pericarp at the mature and ripened stages. Since the signal attenuated with elongation of the diffusion period (Δ), a set of signals, A_0, measured without the pulse magnetic field gradients, and A, measured with the pulse magnetic field gradients, were obtained for each diffusion time. Signal attenuations with pulse gradient magnetic fields, $\ln (A/A_0)$, of the fruits are plotted in Fig. 4. All

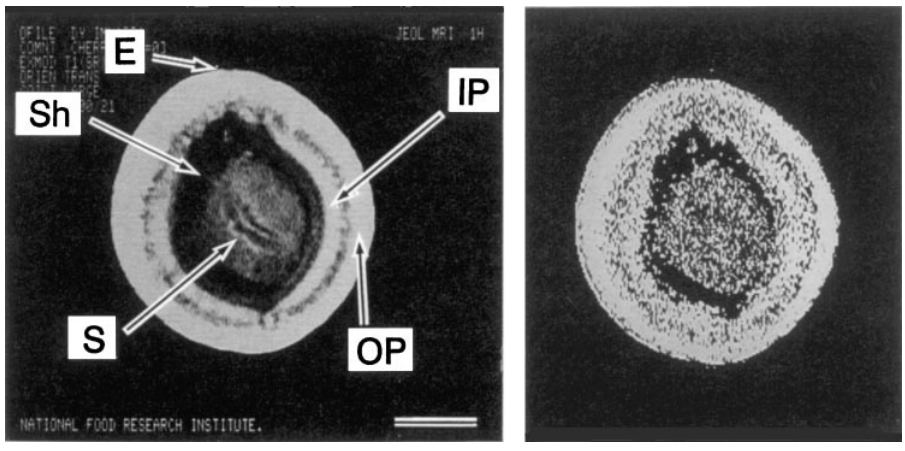

Figure 2. ^{1}H NMR image of a cherry fruit at ripened stage showing anatomy (left) and diffusion coefficient image (right) measured by the pulse gradient spin–echo method[24] ($T_E = 25$ ms, $T_R = 5$ s; pulse sequence is not indicated in Fig. 1). Symbols: S = seed; Sh = shell; IP = inner-side of pericarp; OP = outer-side of pericarp; E = epidermal tissues. The scale bar represents 2 mm. The diffusion coefficient image is normalized based on the maximum diffusion coefficient (1.7×10^{-5} cm^2 s^{-1}).

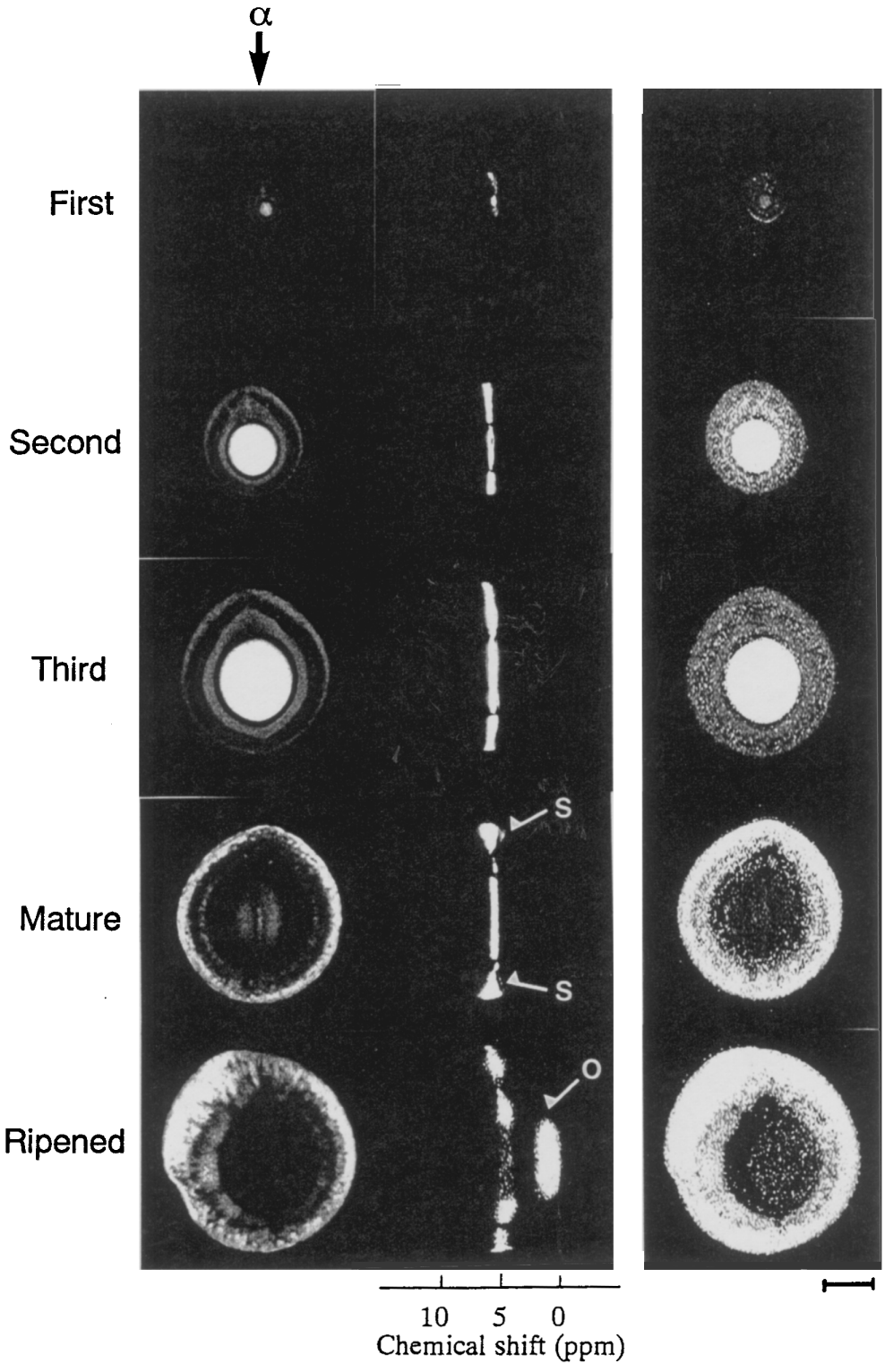

Figure 3. ^{1}H NMR images (left), localized spectral images (center) and T_1 images (right) of growing cherry fruits. ^{1}H NMR images were measured with $T_E = 21$ ms and $T_R = 5$ s. T_1 images were created based on calculated T_1 values using six images measured with varying T_R (0.5, 0.9, 1.2, 1.5, 2.0 and 5.0 s). ^{1}H NMR images and T_1 images were normalized based on the maximum intensity and 3 s, respectively. The vertical arrow at the top (α) indicates the place which was selectively excited in the measurements of the localized spectral images. Arrows s indicate sugars and the arrow o indicates oils. The scale bar represents 2 mm.

the curves are non-linear, indicating that movement of water molecules in the fruits was restricted by cell organization.[21]

The results were treated by using the Meerwall–Ferguson modification[22] of the model of Tanner[21] and diffusion coefficient (D_0), size of compartments in which water molecules freely move (a) and permeability of membrane partitions (P or D_∞/D_0) consisting of the compartments were calculated by a curve-fitting analysis[16] (Table 2).

Table 1. Changes in spin–lattice relaxation times [T_1 (s)] of water in various tissues of cherry fruits

Stage	Seed	Shell	Inner-side of pericarp	Outer-side of pericarp
First	0.81 ± 0.01	0.48 ± 0.08	0.51 ± 0.14	0.44 ± 0.05
Second	1.95 ± 0.07	0.84 ± 0.04	0.81 ± 0.04	0.70 ± 0.03
Third	1.85 ± 0.05	0.95 ± 0.06	0.80 ± 0.08	0.75 ± 0.06
Mature	0.50 ± 0.03	0.52 ± 0.06	1.30 ± 0.11	0.99 ± 0.07
Ripened	0.43 ± 0.05	0.42 ± 0.13	0.93 ± 0.07	1.38 ± 0.09

The diffusion coefficient for the fruits at the first stage was not high (1.3×10^{-5} cm^2 s^{-1}) and reached a maximum comparable to that of pure water (2.14×10^{-5} cm^2 s^{-1} at 25 ± 1 °C)[23] at the second stage. The diffusion coefficient decreased to 1.7×10^{-5} cm^2 s^{-1} at the third stage. The diffusion coefficient was low at the mature stage, 1.0×10^{-5} cm^2 s^{-1}, and increased to 1.6×10^{-5} cm^2 s^{-1} at the ripened stage. The value at the ripened stage corresponds to that in the pericarp obtained by the pulse gradient spin-echo method[24] for another over-mature fruit (1.7×10^{-5} cm^2 s^{-1}) shown in Fig. 2 (right). The compartment size did not change and the membrane permeability seemed to be maintained throughout the growth stages.

^{13}C NMR spectra of 80% ethanol extracts of the pericarps at the mature stage (a) and of an intact fruit (b) and a seed (c) at the ripened stage are shown in Fig.

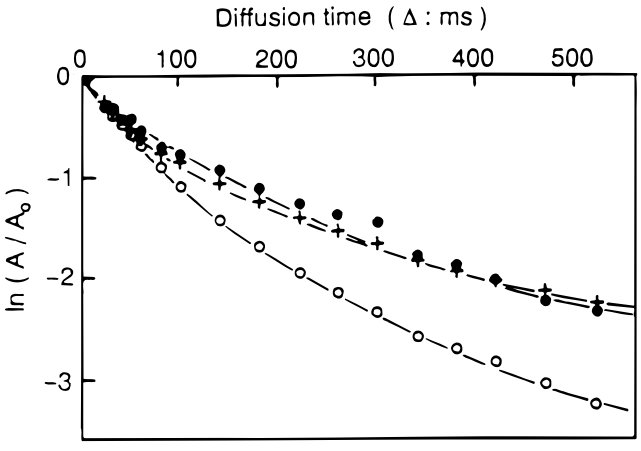

Figure 4. Relationship between the decrease in signal intensity by pulse magnetic field gradients, ln (A/A_0), and diffusion time (Δ). The magnitude of the pulse magnetic field gradients was 140 mT m^{-1} for 3 ms. Symbols indicate (●) the first, (○) the second and (+) the ripened stages.

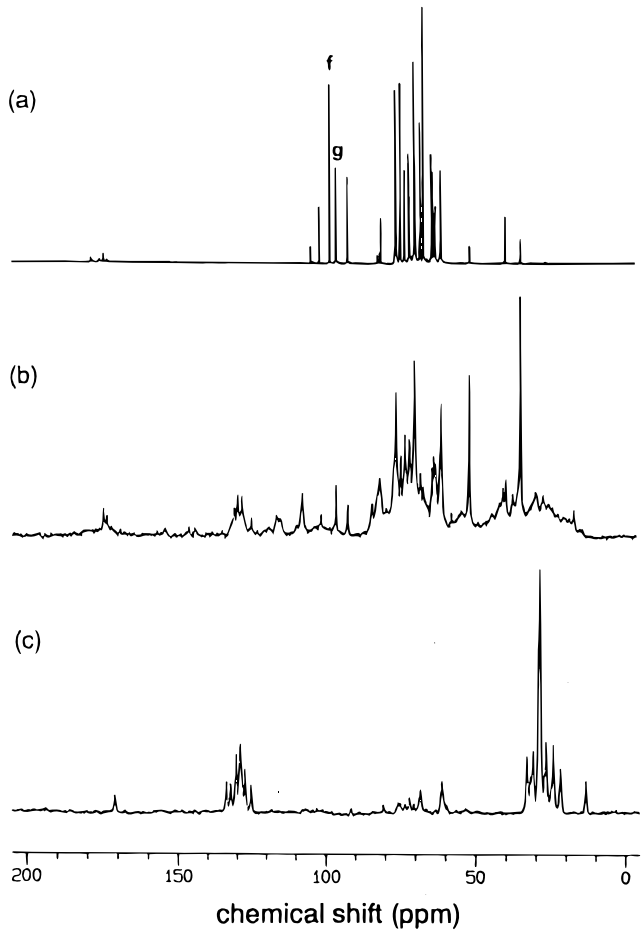

Figure 5. ^{13}C NMR spectra of (a) 80% ethanol extract of pericarp at the mature stage, and (b) an intact fruit and (c) a seed at the ripened stage. Chemical shifts are determined with respect to tetramethylsilane at 0 ppm. Characteristic signals of fructose and glucose are indicated by f and g, respectively.

Table 2. Changes in compartment size (a), permeability (P or D_∞/D_0) and initial diffusion coefficient (D_0) with growth stages of cherry fruits[a]

Stage	a (μm)	P	D_∞/D_0	D_0 (cm^2 s^{-1})
First	35.7 ± 0.1	0.33 ± 0.11	0.25 ± 0.06	$1.3 \pm 0.2 \times 10^{-5}$
Second	34.1 ± 0.6	0.45 ± 0.10	0.31 ± 0.05	$2.1 \pm 0.1 \times 10^{-5}$
Third	35.4 ± 0.1	0.24 ± 0.13	0.19 ± 0.07	$1.7 \pm 0.2 \times 10^{-5}$
Mature	35.7 ± 0.1	0.31 ± 0.13	0.24 ± 0.07	$1.0 \pm 0.3 \times 10^{-5}$
Ripened	35.3 ± 0.1	0.23 ± 0.04	0.19 ± 0.03	$1.6 \pm 0.2 \times 10^{-5}$

[a] The parameters were calculated using von Meerwall and Ferguson's modification[22] of the model of Tanner.[21]

5. Glucose and fructose were detected in the pericarps of the mature stage[25] [Fig. 5(a)], characteristic peaks of which are 96 ppm for glucose and 98 ppm for fructose. In the spectrum of the intact fruit [Fig. 5(b)], peaks around 35 ppm and 52 together with those around 170 ppm are due to aspartic acid[26] and that at 40 ppm to malic acid.[27] Sugars were also detected from 60 to 110 ppm. In the spectrum of the seed [Fig. 5(c)], the peaks at 13 and *ca.* 30 ppm are due to methyl and methylene carbons of fatty acids. The peaks around 130 ppm are due to double bonds and those at 172 ppm are due to carbonyl carbons of the fatty acids. Since glycerol peaks are observed at 62 and 70 ppm, these fatty acids are stored at glycerides.

DISCUSSION

In this investigation, we attempted to examine the physiological and textural changes of sweet cherry fruits during various growth stages by measuring the physical states of cell-associated water by NMR imaging.

The echo time (T_E) used for measurements (21 and 27 ms) were long, and therefore water molecules strongly ordered with the cell constituents and restricted in mobility were not detected. When the image signal became very weak or was not detected, the tissue still contained *ca.* 60% of water on a fresh weight basis in the cherry tissue (Fig. 3, the seed of the ripened stage). This is similar to the results for growing soybean seeds.[28] Only water with high mobility, free water, was detected, which is called simply water here. Hence the signal intensity correlates with the amount of free water. Cell metabolism depends upon transport of substrates and O_2 gas to reaction sites by water. Removal of products and CO_2 gas from reaction sites also occurs by water movement, and exhaust of heat generated with metabolism is carried out through water movement. Therefore, the amount and mobility of free water reflect metabolic activity; when the metabolic rate is high, the amount of water and water mobility are high. On the other hand, when macromolecules such as starch and proteins are accumulated in cells, water molecules are ordered and the mobility is decreased. Therefore, the metabolic rate is at a low level, as observed in mature seeds and storage organs.[28,29] Hence water detection by NMR imaging is very useful in monitoring changes in metabolic activity in tissues.

The seed and pericarp of the sweet cherry fruit (cv. Sato-Nishiki) has different properties with regard to changes of physical states of water (Fig. 3 and Table 1). There were large amounts of water with high mobility in growing seeds. The amount and mobility of water decreased with seed maturation. The tendency was reversed in the pericarp. The amount and mobility of water in the pericarp were low when the seed was growing but increased after seed maturation. This situation is similar to the relationship between the seed and pericarp including dissepiments of tomatoes.[16,30] In the pericarp of the cherry fruit until the third stage, metabolic activity is considered to be suppressed based on the small water content and low mobility. On the other hand, the metabolic activity of the seed is high because the seed contained large amounts of high-mobility water during the stages. In spite of the fact that the pericarp enlarged with seed growth, the metabolic activity of the seed greatly exceeds that of the pericarp. The seed formation, which is a primary object of fruit growth,[31] may require larger amounts of energy than the pericarp tissue enlargement. During seed organization, the pericarp is considered to act as a sort of storehouse where photosynthates are temporarily accumulated for further transportation to the seed. Therefore, the amount and mobility of water are decreased to suppress metabolic activity. The shell maintained water until the third stage, indicating that the shell was also physiologically active.

The accumulation of glucose and fructose (Figs 3 and 5) that occurred in the pericarp corresponded to an increase of water at the mature stage. It was also observed in the fruits of cherry tomato[16] that the sugar content increases just before ripening.[2,32] The accumulation of sugars at this stage is considered to be a result of the decline in the metabolic pathway which produces carbohydrate skeletons for seed formation. Sugars disappeared at the ripened stage and this was associated with a further increase in water (Fig. 3). The increase in organic acid signals in the ^{13}C NMR spectrum of the fruit and the appearance of oil signals in the seed (Figs 3 and 5) indicate that sugars were subjected to a degradation metabolism producing low molecular weight organic acids and oils. Mobile oils detected in the ripened seed are considered to be stored as oil droplets of glycerides like oil seeds.[33–35]

Movement of cell-associated water gives information about the properties of the interface between solid constituents and liquid phases in the tissues. Restricted diffusion of water was measured (Fig. 4 and Table 2). In this experiment, the signals came from a whole sliced section of 1.6 mm thickness. However, based on the Fig. 3, water was mainly present in the seeds for the first, second and third stages, whereas it was observed in the pericarp for the mature and ripened stages. The transport rate of water indicated by the initial diffusion coefficient (D_0) in the seed of the second stage was very high (2.1×10^{-5} cm^2 s^{-1}) (Table 2), comparable to the self-diffusion coefficient of pure water.[23] Taking into account the fact that seed cells have many cell constituents and soluble macrocompounds ordering water molecules, functional movement of membrane structures and elevation of temperature by active degradation metabolism are the reason for such high water movement.[23]

The diffusion coefficient decreased to 80% of the maximum at the third stage. This is considered to indicate a decline of metabolic activity and the accumulation of macromolecules after the establishment of cell structures in the seed. The diffusion coefficient of water in the pericarp increased from 1.0×10^{-5} to 1.6×10^{-5} cm^2 s^{-1} during ripening; the water content also increased. This may be due to the fact that well differentiated cell organization in the pericarp is no longer necessary in association with the termination of the physiological roles to sustain seed formation. Stored macromolecules were degraded to low molecular weight compounds and osmosis increased (Fig. 5).[36] Consequently, water motion is released from restriction, water intrudes into cells from outside and the pericarp loses

its firmness.[2,3] The mature stage seems to be suitable for harvesting because sugars were detected (Fig. 3) and the firmness was still maintained.

The compartment size (a) and permeability (P or D_∞/D_0) of membrane partitions characterize the structural organization of the networks in the tissues (Table 2). These values were expected to alter with growth stages because the fruits were enlarging, and the amount of accumulated materials were fluctuating. However, they did not change significantly throughout the growth stages. The compartment size (35 μm) and permeability (20–30%) are close to those obtained in growing barley seeds.[23] Although there is no substantial evidence, it may be that to maintain equilibration between the compartments in the tissues, uniform partitions with similar size and permeability are preferable. Only the transport rate (D_0) changed in close relation to the fruit growth. To establish the involvement of these parameters more precisely, individual organs, at least seed, shell and the outer- and inner-sides of the pericarp showing different properties on the ^{1}H NMR images, localized spectral images and T_1 images (Fig. 3) should be measured separately.

The seed and the pericarp were shown to have contradictory properties in relation to water status (Fig. 2 and Table 1). It is suggested that the metabolic rate of the pericarp is suppressed by the accumulation of macromolecular materials during seed formation, which are released at seed maturation (Fig. 3 and Table 2). After the decline in metabolic activity of the seed by maturation, in the pericarp, sugars were at first accumulated but subsequently degraded associated with swelling of parenchyma cells (Figs 3 and 5). Over-maturation may result in loss of sweetness and firmness of the fruit. The nature of the pericarp is an important factor to be taken into account in sweet cherry cultivation. We consider that NMR imaging is a suitable means for monitoring the change of fruit conditions in relation to physiology.

Acknowledgements

The authors thank Drs K. Tanaka and M. Yamaguchi of the National Institute of Fruit Science and Drs M. Nakajima and T. Nakamura of the National Food Research Institute for valuable advice.

REFERENCES

1. T. Suzuki, in *Kaju Engei Daijiten* (*Comprehensive Handbook of Fruit Trees*), edited by K. Sato, H. Mori, O. Matsui, H. Kitajima and T. Chiba, pp. 750–767. Yokendo, Tokyo (1980).
2. S. R. Drake and J. K. Fellman, *HortScience* **22**, 283 (1987).
3. B. Fils-Lycaon and M. Buret, *HortScience* **25**, 777 (1990).
4. P. Mansfield and I. L. Pykett, *J. Magn. Reson.* **29**, 355 (1978).
5. K. H. Hausser and H. R. Kalbitzer, *NMR in Medicine and Biology*. Springer, Berlin (1991).
6. J. S. Clegg, in *Cell-Associated Water*, edited by W. Drost-Hansen and J. S. Clegg, pp. 363–413. Academic Press, New York (1979).
7. C. F. Hazlewood, in *Cell-Associated Water*, edited by W. Drost-Hansen and J. S. Clegg, pp. 165–259. Academic Press, New York (1979).
8. M. Faust, D. Liu, M. M. Millard and G. W. Stutte, *HortScience* **26**, 887 (1991).
9. A. A. Gardea, L. S. Daley, R. L. Kohnert, A. H. Soeldner, L. Ning, P. B. Lombard and A. N. Azarenko, *Sci. Hort.* **56**, 339 (1994).
10. S. Y. Wang, P. C. Wang and M. Faust, *Sci. Hort.* **35**, 227 (1988).
11. C. Y. Wang and P. C. Wang, *HortScience* **24**, 106 (1989).
12. J. M. Pope, in *Magnetic Resonance Microscopy*, edited by B. Blümich and W. Kuhn, pp. 441–457. VCH, Weinheim (1992).
13. P. T. Callaghan, K. W. Jolley and R. S. Humphrey, *J. Colloid Interface Sci.* **93**, 521 (1983).
14. P. T. Callaghan, *Principles of Nuclear Magnetic Resonance Microscopy*. Clarendon Press, Oxford (1991).
15. A. Ohtsuka, T. Watanabe and T. Suzuki, *Carbohydr. Polym.* **25**, 95 (1994).
16. N. Ishida, M. Koizumi and H. Kano, *Sci. Hort.* **57**, 335 (1994).
17. L. Sonego, R. Ben-Arie, J. Raynal and J. C. Pech, *Postharvest Biol. Technol.* **5**, 187 (1995).
18. N. Ishida, H. Kano, H. Hayashi and H. Ogawa, *Anal. Sci.* **7**(Suppl.), 817 (1991).
19. T. C. Farrar and E. D. Becker, *Pulse and Fourier Transform NMR*. Academic Press, New York (1971).
20. S. I. Cho, V. Bellon, T. M. Eads, R. L. Stroshine and G. W. Krutz, *J. Food Sci.* **56**, 1091 (1991).
21. J. E. Tanner, *J. Chem. Phys.* **69**, 1748 (1978).
22. E. von Meerwall and R. D. Ferguson, *J. Chem. Phys.* **74**, 6956 (1981).
23. N. Ishida, H. Ogawa and H. Kano, *Magn. Reson. Imaging* **13**, 745 (1995).
24. E. O. Stejskal and J. E. Tanner, *J. Chem. Phys.* **42**, 288 (1965).
25. G. C. Whiting, in *The Biochemistry of Fruits and Their Products*, edited by A. C. Hulme, Vol. I, pp. 1–31. Academic Press, London (1970).
26. L. F. Burroughs, in *The Biochemistry of Fruits and Their Products*, edited by A. C. Hulme, Vol. I, pp. 119–146. Academic Press, London (1970).
27. R. J. Romani and W. G. Jennings, in *The Biochemistry of Fruits and Their Products*, edited by A. C. Hulme, Vol. II, pp. 411–436. Academic Press, London (1971).
28. H. Kano, N. Ishida, T. Kobayashi and M. Koizumi, *Jpn. J. Crop Sci.* **59**, 503 (1990).
29. N. Ishida, H. Kano, T. Kobayashi, H. Hamaguchi and T. Yoshida, *Agric. Biol. Chem.* **51**, 301 (1987).
30. N. Ishida, T. Kobayashi, M. Koizumi and H. Kano, *Agric. Biol. Chem.* **53**, 2363 (1989).
31. J. C. Crane, *Annu. Rev. Plant Physiol.* **15**, 303 (1964).
32. S. Yamaki, I. Kajiura and N. Kakiuchi, *Bull. Fruit Tree Res. Stn.* **A6**, 15 (1979).
33. J. Schaefer and E. O. Stejskal, *J. Am. Oil Chem. Soc.* **51**, 210 (1974).
34. M. Yoshida, H. Kano, N. Ishida and T. Yoshida, *Agric. Biol. Chem.* **53**, 1395 (1989).
35. M. Koizumi, N. Ishida and H. Kano, *Biosci. Biotechnol. Biochem.* **59**, 2321 (1995).
36. B. G. Coombe, *Annu. Rev. Plant Physiol.* **27**, 507 (1976).

